References

Berg, H. C. & Purcell, E. M. 1977. Physics of chemoreception. *Biophysical journal*, **20**, 193–219. doi:10.1016/S0006-3495(77)85544-6.

Goodhill, G. & Urbach, J. 1999. Theoretical analysis of gradient detection by growth cones. *Journal of neurobiology*, pages 230–241.

Kaizu, K., de Ronde, W., Paijmans, J., Takahashi, K., Tostevin, F. & ten Wolde, P. R. 2014. The Berg-Purcell Limit Revisited. *Biophysical Journal*, **106**, 976–985. doi:10.1016/j.bpj.2013.12.030.

Kulesa, P. M., Teddy, J. M., Stark, D. A., Smith, S. E. & McLennan, R. 2008. Neural crest invasion is a spatially-ordered progression into the head with higher cell proliferation at the migratory front as revealed by the photoactivatable protein, KikGR. *Developmental Biology*, **316**, 275–87. doi:10.1016/j.ydbio.2008.01.029.

Mac Gabhann, F., Ji, J. W. & Popel, A. S. 2006. Computational model of vascular endothelial growth factor spatial distribution in muscle and pro-angiogenic cell therapy. *PLoS computational biology*, **2**, e127. doi:10.1371/journal.pcbi.0020127.

Mac Gabhann, F. & Popel, A. 2005. Differential binding of VEGF isoforms to VEGF receptor 2 in the presence of neuropilin-1: a computational model. *American Journal of Physiology- ...*, **21205**, 2851–2860. doi:10.1152/ajpheart.01218.2004..

McLennan, R., Dyson, L., Prather, K. W., Morrison, J. A., Baker, R. E., Maini, P. K. & Kulesa, P. M. 2012. Multiscale mechanisms of cell migration during development: theory and experiment. *Development*, **139**, 2935–44. doi:10.1242/dev.081471.

McLennan, R. & Kulesa, P. M. 2010. Neuropilin-1 interacts with the second branchial arch microenvironment to mediate chick neural crest cell dynamics. *Developmental dynamics : an official publication of the American Association of Anatomists*, **239**, 1664–73. doi:10.1002/dvdy.22303.

McLennan, R., Teddy, J. M., Kasemeier-Kulesa, J. C., Romine, M. H. & Kulesa, P. M. 2010. Vascular endothelial growth factor (VEGF) regulates cranial neural crest migration in vivo. *Developmental Biology*, **339**, 114–25. doi:10.1016/j.ydbio.2009.12.022.

Ridenour, D. a., McLennan, R., Teddy, J. M., Semerad, C. L., Haug, J. S. & Kulesa, P. M. 2014. The neural crest cell cycle is related to phases of migration in the head. *Development (Cambridge, England)*, **141**, 1095–103. doi:10.1242/dev.098855.

Streichan, S. J., Valentin, G., Gilmour, D. & Hufnagel, L. 2011. Collective cell migration guided by dynamically maintained gradients. *Physical Biology*, **8**, 045004. doi:10.1088/1478-3975/8/4/045004.

Teddy, J. M. & Kulesa, P. M. 2004. In vivo evidence for short-and long-range cell communication in cranial neural crest cells. *Development*, **131**, 6141–51. doi:10.1242/dev.01534.

Vempati, P., Popel, A. S. & Mac Gabhann, F. 2011. Formation of VEGF isoform-specific spatial distributions governing angiogenesis: computational analysis. *BMC Systems Biology*, **5**, 59. doi:10.1186/1752-0509-5-59.

Yen, P., Finley, S. D., Engel-Stefanini, M. O. & Popel, A. S. 2011. A two-compartment model of VEGF distribution in the mouse. *PloS one*, **6**, e27514. doi:10.1371/journal.pone.0027514.

S1 Supplementary Information

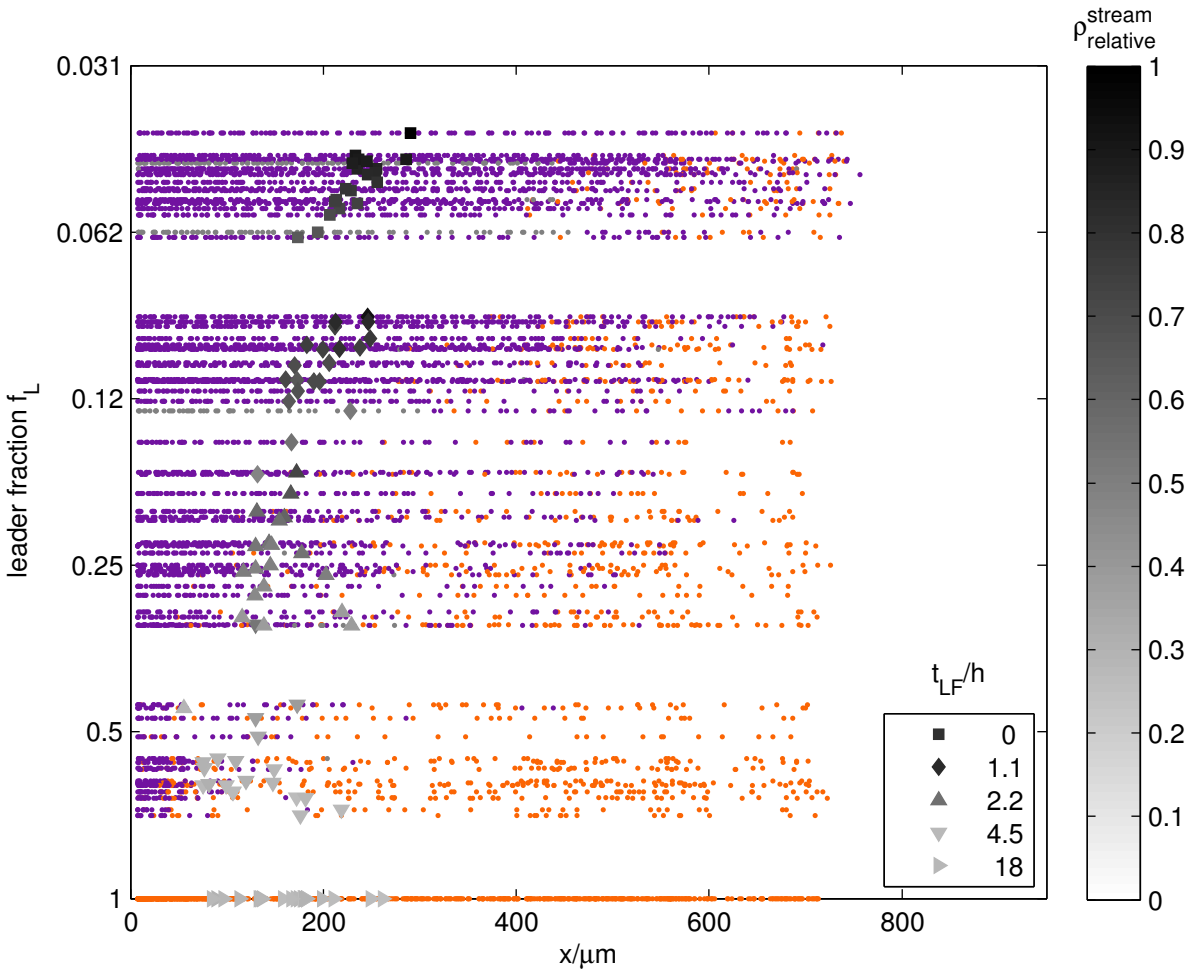

Figure S1: **Supplementary results.** Same data as in Fig. 2, but now the x-positions for each individual simulation are plotted against each leader fraction f_L, the latter now not being averaged.

S1.1 Derivation of sensing accuracy

Berg & Purcell (1977) derive a fundamental biophysical limit to accuracy with which a cell can sense a chemical gradient. We briefly outline their derivation here, before commenting on parameterisation.

The limit in sensing accuracy is due to fluctuations in low numbers of molecules, and will be derived for the case of a perfect sensor. First, let us consider the assumptions underlying this approximation in the case of a cell.

S1.1.1 The flux of chemical onto a cell partially covered with absorbing receptors can be near optimal.

Let the evolution of a chemical substance of concentration c, with diffusivity D, be described by the diffusion equation:

$$D\nabla^2 c = \frac{\partial c}{\partial t} \tag{1}$$

If we assume cells to be spheres of radius R, and the bulk concentration far away from the cell, c_∞, to be constant[1], then the flux onto the surface of the cell is given by

$$J = 4\pi D c_\infty R \tag{2}$$

From this, one can calculate the probability that a randomly diffusing molecule at a distance r from the cell will eventually be absorbed to be

$$P = R/r \tag{3}$$

If we assume the cell surface is only absorbing, but perfectly so, on N receptor patches of size s, and if these patches cover a small area fraction of the cell surface, the modified flux is given by

$$J = 4\pi D c_\infty \frac{Ns}{Ns + \pi R} \tag{4}$$

Thus we can get near the maximum flux even with a low area fraction, i.e., there are diminishing returns of having ever more receptors (of the same kind) on the cell surface. If the receptors aren't peferctly absorbing, i.e., there is a probability $p < 1$ that a molecule will bind to the receptor, Berg & Purcell (1977) make the case that diffusing molecule will stay close to the receptor after an unsuccessful binding event and thus get repeated chances of binding. Note we have also ignored the possibility of a receptor being occupied by a bound molecule, i.e., we assume fast internalisation of receptor-ligand complexes.

S1.1.2 Sensing limit of a perfect instrument

The fluctuations in particle number N are proportional to $1/\sqrt{N}$. Let a perfect sensor be counting molecules in a volume V with background (or average) concentration $\bar{c}$. The inaccuracy in a single concentration measurement will be

$$\frac{\Delta c}{\bar{c}} \approx \frac{1}{\sqrt{N}} = \frac{1}{\sqrt{V\bar{c}}} \tag{5}$$

in three dimensions, or $1/\sqrt{A\bar{c}}$ in two dimensions. The count of molecules can be improved by repeated measurements. In a time T our perfrect instrument can make $TD/V^{2/3}$ independent measurements, based on the timescale of a molecule diffusing through the measurement volume V. Thus, with $V \sim R^3$, the measurement uncertainty reduces to

$$\frac{\Delta c}{\bar{c}} \approx \frac{1}{\sqrt{DT\bar{c}R}} \tag{6}$$

in three dimensions, or $\Delta c/\bar{c} \approx 1/\sqrt{DT\bar{c}}$ in two dimensions. The exact derivation introduces a numerical factor of

[1]This assumption may be violated with tissue growth, but should hold on the short time scales considered here.

order unity, but since we can only parameterise the sensing accuracy to orders of magnitude, we will ignore this.

Kaizu *et al.* (2014) revisit the Berg-Purcell limit and derive corrections to the sensing limit by considering diffusive ligand transport as well as receptor binding kinetics. Since we assume our reactions to be diffusion limited, these corrections do not apply. Similarly, one can correct for movement of the cell relative to the medium to derive the apparent gradient seen by the cell and its detection limit, but we assume this to be neglible.

S1.1.3 Parameterisation of the sensing accuracy for neural crest cells

Most of the variables upon which the sensing accuracy depends are underdetermined in the case of chick cranial neural crest migration, such as VEGF diffusivity D, VEGF background concentration $\bar{c}$ and the sensing time T. Nevertheless, we can proceed to make order of magnitude estimates, which can serve as bounds for our model simulations.

The concentration of VEGF used in *in vitro* experiments is 1μg/ml (50mM), which at a molecular weight of 19.2kDa $\approx$ 20kg/mol, leads us to estimate $\bar{c} \approx 0.3 \cdot 10^8/\mu\text{m}^3$.

The timestep of our simulations is $\Delta t = 1$min, and we assume that only a fraction of it is taken up with sensing, and most of it with movement. We could there for estimate $T \leq 0.1 \cdot \Delta t = 0.1$min. If we relax our assumptions this estimate might change by an order of magnitude, which would only change the sensing accuracy by a factor of roughly 1/3, which will give qualitatively similar results in typical model simulations.

For the measurement of a gradient, i.e., the difference between two concentration measurements, the Berg-Purcell limit (6) will increase by a factor of $\sqrt{2}$ (Goodhill & Urbach 1999). With the estimates for $\bar{c}$ and T as above, and the parameter values $D = 0.1\mu\text{m}^2/\text{h}$ and $R = 7.5\mu$m (Table 1), we get an estimate of the sensing accuracy (6) of $\Delta c/c \approx 0.002$ in three dimensions, or $\Delta c/c \approx 0.01$ in two dimensions. These can be taken as a lower bound for the (order of magnitude of) sensing accuracy of neural crest cells in our model.

Table 1: **Model parameters used.**
Parameter values listed were used as a default, unless otherwise stated. Where a range is given, the model gives qualitatively similar results within that range, and the italicised value is the one used for the figures in this paper.

	Description	Value	Reference
t_{LF}	time[1] after which newly inserted cells are followers	0h	Fig. 2
n_{filo}	directions sampled[2] per timestep	2	n/a
Δt	simulation time step	1 min	n/a
R	cell radius (nuclear)	7.5μm	McLennan & Kulesa (2010)
v_{lead}	cell speed (leader cells)	41.6μm/h	Kulesa *et al.* (2008)
v_{follow}	cell speed (follower cells)	49.9μm/h	Kulesa *et al.* (2008)
L_y	height of migratory domain	120μm	McLennan *et al.* (2012)
L_x	length of migratory domain (grows logistically)	300μm to 1100μm	McLennan *et al.* (2012)
l_{filo}	sensing radius (cell radius + twice mean filopodial length)[3]	27.5μm	unpublished, Kulesa *et al.*
$l_{\mathrm{filo}}^{\mathrm{max}}$	maximum cell separation before contact is lost	45μm	unpublished, Kulesa *et al.*
$\Delta c/c$	sensing accuracy	0.001 to *0.1*	Section S1.1
D	diffusion coefficient of chemoattractant (effective)	0.1μm^2/h	see notes
χ	production rate of chemoattractant	0.0001/h	see notes
λ	chemoattractant internalisation rate	100 to *1000*/h	see notes
k_{in}	rate at which cells enter the domain	10/h	see notes

Notes

Diffusion coefficient of chemoattractant, D: The primary identified chemoattractant in chick cranial neural crest migration is VEGF^{165} (McLennan *et al.* 2010). Its related isoform VEGF^{164} is known to bind to extracellular matrix (ECM), and studies in angiogenesis estimate as little as 1% of it may be freely diffusing, the rest bound to ECM and cellular receptors (Mac Gabhann *et al.* 2006). Hence, we choose a low effective diffusivity.

Production rate of chemottractant, χ: In other tissues, VEGF production, or estimates thereof, range from 0.01-0.20 molecules/cell/s (Yen *et al.* 2011), 4.39-5.27$\cdot 10^{-5}$molecules/μm$^-2$/s (Vempati *et al.* 2011) to $0.25 \cdot 10^{-17}$pmol/μm^2/s(Mac Gabhann *et al.* 2006). In our system, the rate of VEGF production is unknown and difficult to measure. Howeever, it is outweighed by internalisation through migrating neural crest cells, as VEGF is not seen to be replenished in trailing portions of the stream (McLennan *et al.* 2010). Thus, we assume χ to be low.

Chemoattractant internalisation rate, λ: To our knowledge, no estimates or measurements of VEGF internalisation rate of chick cranial neural crest exists. Angiogenesis studies have used values of $k_{\mathrm{VEGFR2}} = O(10^{-4})$/s (Mac Gabhann & Popel 2005, Yen *et al.* 2011). Berg & Purcell (1977) estimate the number of receptors needed for a near-optimal sensing accuracy as $N_R = R/s$, where R is the cell radius and s the receptor size. With $s = O(\mathrm{nm})$, we can estimate the number of receptors to be $N_R \geq 10^4$. If receptor internalisation rates are comparable to other tissues, a lower bound on λ would be given by $k_{\mathrm{VEGFR2}} N_R > 1$. However, the concentration of VEGF in our system is unknown, and hence the units of c, and therefore λ, in our model are arbitrary. We assume a high λ to ensure readily consumption of chemoattractant by cells.

Rate at which cells enter the domain, k_{in}: This is the rate of attempted cell insertions, in a typical simulation $O(10\%)$ of insertions are unsuccessful. It should be noted here again that our simulations are a two-dimensional abstraction of the three-dimensional migratory stream, which may contain 4-5 times as many cells *in vivo* in the transverse (z) direction.

[1]Time t_{LF} is taken after start of migration, which is 6 hours after electroporation, i.e., experimental $t = 0$.

[2]This is not directly relatable to the number of filopodia, which are greater in number, but sample at a lower speed (McLennan *et al.* 2012).

[3]As we have only implemented contact between filopodium and cell body, but not between two filopodia, which does occur *in vivo* (Teddy & Kulesa 2004), we allow for a greater effective length.